

Efficient visible to infrared quantum cutting through downconversion with the Er³⁺–Yb³⁺ couple in Cs₃Y₂Br₉

J. J. Eilers,¹ D. Biner,² J. T. van Wijngaarden,¹ K. Krämer,² H.-U. Güdel,² and A. Meijerink^{1,a)}

¹Debye Institute, Utrecht University, Princetonplein 5, 3584 CC Utrecht, The Netherlands

²Department of Chemistry, University of Bern, Freiestrasse 3, CH-3000 Bern 9, Switzerland

(Received 22 February 2010; accepted 8 March 2010; published online 14 April 2010)

Downconversion of one visible photon to two near-infrared photons may increase the efficiency of c-Si solar cells by 30%. The lanthanide ion couple Er³⁺–Yb³⁺ is well known for efficient upconversion but for the reverse process, downconversion, fast multiphonon relaxation from the ⁴F_{7/2} level has been shown to compete with downconversion. Here we report efficient downconversion for the Er–Yb couple in Cs₃Y₂Br₉. The low phonon energy in this bromide host suppresses multiphonon relaxation and efficient two step energy transfer from the ⁴F_{7/2} level of Er³⁺ is observed and results in strong 1000 nm emission from Yb³⁺. Based on emission spectra and luminescence life time measurements an intrinsic downconversion efficiency close to 200% is determined. © 2010 American Institute of Physics. [doi:10.1063/1.3377909]

The efficiency of solar cells is limited to ~30% (the Shockley–Queisser limit) largely due to spectral mismatch losses: Low energy (sub-band gap) photons are not absorbed (transmission losses) while high energy photons produce a “hot” electron-hole pair that relaxes to the band edges (thermalisation losses). To reduce these losses, both downconversion and upconversion materials may be applied. Two seminal papers by Trupke, Green, and Würfel^{1,2} demonstrated that ideal upconversion or downconversion materials raise the theoretical limit efficiency for a single junction solar cell to ~50% and 40%, respectively. Since then, the search for efficient up- and downconversion materials has intensified.^{3,4} A promising class of materials are lanthanide doped phosphors, both for up- and downconversion. The rich energy level structure of lanthanide ions and the sharp atomiclike transitions allow for quantum cutting on a single ion, by sequential two-step emission, or in a pair of ions, through downconversion.^{3,4} Efficient downconversion for solar cells has been reported for the Tb–Yb and the Pr–Yb couples.^{4–7} The well-known upconversion couple Er–Yb can in principle also give rise to efficient downconversion.^{8,9} The Er³⁺ ion has excited states around 20 000 cm⁻¹ (⁴F_{7/2}) and 10 000 cm⁻¹ (⁴I_{11/2}) allowing for a two-step energy transfer process raising two Yb³⁺ neighbors to the ²F_{5/2} excited state around 10 000 cm⁻¹. Upon excitation in the ⁴F_{7/2} level cross-relaxation can occur, Er³⁺ (⁴F_{7/2} → ⁴I_{11/2}), Yb³⁺ (²F_{7/2} → ²F_{5/2}), followed by a second energy transfer step from the ⁴I_{11/2} level of Er³⁺ raising a second Yb³⁺ ion to the ²F_{5/2} excited state. Both Yb³⁺ ions can emit a ~1000 nm photon that can be absorbed by a c-Si solar cell.

Previous work on the Er–Yb couple in fluoride and chloride host materials demonstrated that multiphonon relaxation from the ⁴F_{7/2} to the ²H_{11/2} and ⁴S_{3/2} level is faster than cross-relaxation with a neighboring Yb³⁺ and as a result the downconversion efficiency is very low.^{8,9} The remedy for fast multiphonon relaxation is reduction of the maximum phonon energy. Multiphonon relaxation becomes very slow

(slower than radiative decay or nearest neighbor energy transfer) when the gap exceeds five phonons. For Er³⁺ the gap between the ⁴F_{7/2} level and the next lower ²H_{11/2} level is approximately 1250 cm⁻¹ (Refs. 8–10) and in a bromide host the maximum phonon energy is ~180 cm⁻¹ (Refs. 10–12) which results in a long lived ⁴F_{7/2} state. Indeed, ⁴F_{7/2} emission from Er³⁺ has been observed in bromides.^{10,11} Here we will demonstrate that in a bromide host efficient downconversion from the ⁴F_{7/2} level is possible in the Er³⁺–Yb³⁺ couple.

Single crystals of Cs₃Y₂Br₉ doped with Er³⁺ (1%) or Er³⁺ (1%) and Yb³⁺ (15%) were grown by the vertical Bridgeman technique as described in Refs. 10–14. High quality transparent single crystals were obtained. All dopant concentrations are given as mole percent with respect to Y³⁺. Luminescence spectra were recorded with an Edinburgh Instruments FLS 920 spectrofluorometer set-up described in Refs. 7–9. In this set-up laser excitation is possible with a Lambda Physik LPD3000 dye laser pumped by a LPX100 XeCl Excimer laser. In the present experiments, a Coumarin 102 dye was used for (ns pulsed) excitation around 490 nm.

To determine if multiphonon relaxation from the ⁴F_{7/2} level is indeed slow, an emission spectrum was recorded upon (dye laser) excitation at 489.7 nm in the ⁴F_{7/2} level. In Fig. 1 the emission spectrum is shown. The spectrum shows strong ⁴F_{7/2} emission lines, corresponding to transitions to both the ⁴I_{15/2} ground state and the ⁴I_{13/2} level. This is in line with earlier observations of ⁴F_{7/2} emission for Er³⁺ in bromides. Also weak emission from the ²H_{11/2}, ⁴S_{3/2}, and ⁴F_{9/2} levels is observed. These lower energy levels can be populated both by radiative and nonradiative decay from the ⁴F_{7/2} level. The observation of ⁴F_{7/2} emission shows that downconversion from this level can be expected upon codoping with Yb³⁺.

In Fig. 2 the emission spectra for Cs₃Y₂Br₉ doped with Er³⁺ (1%) and codoped with Er³⁺ (1%) and Yb³⁺ (15%) are shown for ⁴F_{7/2} excitation at 490 nm. For the Er³⁺-doped sample three characteristic Er³⁺ emission peaks are observed originating from the ⁴I_{11/2}, the ⁴S_{3/2} and the ⁴I_{13/2} level (assignment is given in Fig. 2). When 15% Yb is incorporated

^{a)}Author to whom correspondence should be addressed. Electronic mail: a.meijerink@uu.nl.

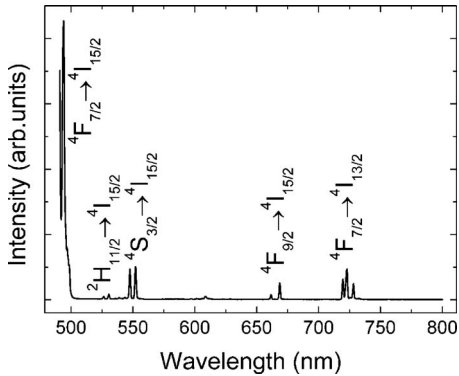


FIG. 1. Emission spectrum of $\text{Cs}_3\text{Y}_2\text{Br}_9$:1%Er upon excitation into the Er^{3+} $4\text{F}_{7/2}$ level at 489.7 nm $T=4.4$ K.

[Fig. 2(b)] the Er^{3+} emission lines in the near-infrared (NIR) are no longer observed and the emission spectrum only shows Yb^{3+} emission around 1000 nm. The observation of this emission upon excitation into the Er^{3+} $4\text{F}_{7/2}$ level, shows that there is energy transfer from the Er^{3+} $4\text{F}_{7/2}$ level to the Yb^{3+} . Furthermore, the absence of $4\text{S}_{3/2}$ emission in Fig. 2(b) indicates that downconversion from the Er^{3+} $4\text{F}_{7/2}$ level dominates over relaxation (radiative or nonradiative) from the Er^{3+} $4\text{F}_{7/2}$ level to lower energy levels. Clearly, all the excitation energy is efficiently transferred from Er^{3+} to Yb^{3+} as no Er^{3+} emission is observed in the sample codoped with 15% Yb^{3+} . Figure 2(c) shows the emission spectrum for the codoped sample at 4 K. The positions of the sharp Yb^{3+} emission lines are consistent with the spectra and energy levels reported for Yb^{3+} in this host lattice in the literature. The absence of Er^{3+} emission (from the $4\text{I}_{11/2}$ or $4\text{F}_{7/2}$ level) shows that also at low temperatures the $\text{Er}^{3+}\rightarrow\text{Yb}^{3+}$ energy transfer is efficient.

Further evidence for downconversion is obtained from Fig. 3 where the excitation spectrum for Yb^{3+} $2\text{F}_{5/2}$ emission around 1000 nm is shown for $\text{Cs}_3\text{Y}_2\text{Br}_9$: 1%Er; 15%Yb at 4 K. The excitation spectrum shows a strong band in the UV with an onset at 380 nm and a sharp peak at 490 nm. The sharp peak is assigned to the $4\text{I}_{15/2}\rightarrow 4\text{F}_{7/2}$ transition. The presence of this peak in the excitation spectrum of the Yb^{3+} emission shows that excitation into the $4\text{F}_{7/2}$ is followed by energy transfer to Yb^{3+} , as expected. Equally interesting is the absence of any other Er^{3+} excitation line. Clearly, for the other energy levels energy transfer to Yb^{3+} is not possible.

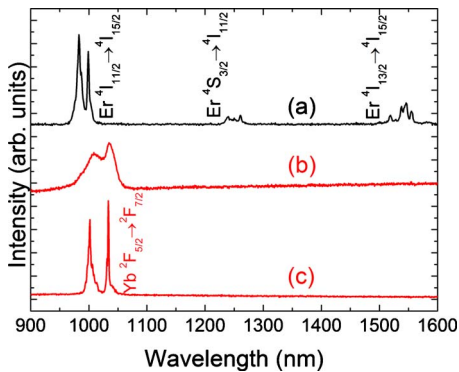


FIG. 2. (Color online) Infrared emission spectrum of (a): $\text{Cs}_3\text{Y}_2\text{Br}_9$:1%Er; $T=300$ K, (b): $\text{Cs}_3\text{Y}_2\text{Br}_9$:1%Er;15%Yb; $T=300$ K and (c): $\text{Cs}_3\text{Y}_2\text{Br}_9$:1%Er;15%Yb; $T=4$ K. The spectra are recorded for excitation into the $4\text{F}_{7/2}$ level of Er^{3+} at 490 nm.

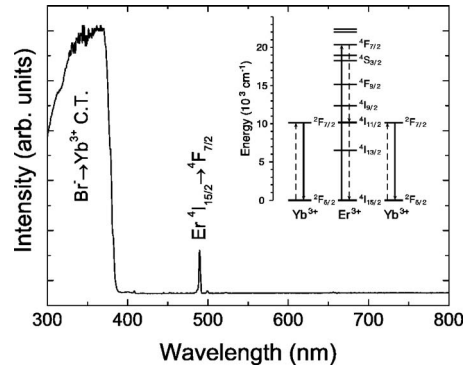


FIG. 3. Excitation spectrum of $\text{Cs}_3\text{Y}_2\text{Br}_9$:1%Er;15%Yb for Yb^{3+} $2\text{F}_{7/2}$ emission at 999 nm, $T=4.4$ K. The inset shows the energy level diagrams of Er^{3+} and Yb^{3+} and the downconversion process is depicted. Broken lines indicate energy transfer while the drawn lines depict radiative decay.

This is different from the observations for the Er–Yb couple in fluorides and chlorides where many Er^{3+} transitions were observed in the excitation spectrum of the Yb^{3+} emission for the codoped samples.^{8,9} A close inspection of the energy levels diagrams as reported for Er^{3+} and Yb^{3+} in the related system $\text{Cs}_3\text{Lu}_2\text{Br}_9$ (Refs. 10–14) shows that the energy difference between the $2\text{F}_{7/2}(0)$ and the $2\text{F}_{5/2}(0)$ crystal field levels of Yb^{3+} is resonant with the energy difference between the $4\text{F}_{7/2}(0)$ and $4\text{I}_{11/2}(4)$ crystal field levels of Er^{3+} . The energy levels for Er^{3+} in $\text{Cs}_3\text{Lu}_2\text{Br}_9$ are very similar to $\text{Cs}_3\text{Y}_2\text{Br}_9$ (shifts of ~ 10 cm^{-1} higher energies are observed for the $4\text{F}_{7/2}$ crystal field components). As a result, resonant cross relaxation is possible in $\text{Cs}_3\text{Y}_2\text{Br}_9$: Er^{3+} , Yb^{3+} and is expected to be efficient down to the lowest temperatures, in agreement with the present observations. Alternative, resonant energy transfer could also occur from the $4\text{F}_{7/2}$ level of Er^{3+} to a double excited state in an exchange-coupled pair of Yb^{3+} ions. Based on the present results we cannot distinguish between the two processes. Cross-relaxation from any of the other Er^{3+} levels between 12 000 and 25 000 cm^{-1} requires phonon assistance. From the reported energy level structure and the present measurements, the energy mismatch for Er^{3+} ($2\text{H}_{11/2}\rightarrow 4\text{I}_{13/2}$), Yb^{3+} ($2\text{F}_{7/2}\rightarrow 2\text{F}_{5/2}$) cross-relaxation is determined to be ~ 1900 cm^{-1} while the ($4\text{S}_{3/2}\rightarrow 4\text{I}_{13/2}$), Yb^{3+} ($2\text{F}_{7/2}\rightarrow 2\text{F}_{5/2}$) and ($4\text{F}_{5/2}\rightarrow 4\text{I}_{11/2}$), Yb^{3+} ($2\text{F}_{7/2}\rightarrow 2\text{F}_{5/2}$) cross-relaxation processes both have a mismatch of ~ 1150 cm^{-1} . In view of the low maximum phonon energy of 180 cm^{-1} these transfer processes require emission of more than five phonons and are therefore not efficient. The strong and broad excitation band below 380 nm is assigned to an interconfigurational charge transfer transition (CT) on Yb^{3+} . Excitation in the CT band is followed by fast nonradiative relaxation to both the $2\text{F}_{5/2}$ and $2\text{F}_{7/2}$ levels of Yb^{3+} .¹⁵ Relaxation to the $2\text{F}_{5/2}$ level is followed by $2\text{F}_{5/2}\rightarrow 2\text{F}_{7/2}$ emission around 1000 nm. Because of the higher oscillator strength of the fully allowed CT transition, this band is much stronger than the parity forbidden $4f\rightarrow 4f$ transition on Er^{3+} .

Figure 4 shows excitation spectra for Er^{3+} $4\text{I}_{13/2}$ emission at 1548 nm in $\text{Cs}_3\text{Y}_2\text{Br}_9$:1%Er (a) and $\text{Cs}_3\text{Y}_2\text{Br}_9$:1%Er; 15%Yb (b) at 4 K. Figures 4(a) and 4(b) show a number of excitation peaks, each corresponding to the excitation of a different excited state of the Er^{3+} ion. Emission from the $4\text{I}_{13/2}$ level is observed due to population of the $4\text{I}_{13/2}$ level by radiative transitions to this level or cross-relaxation processes between Er^{3+} neighbors. A remarkable difference be-

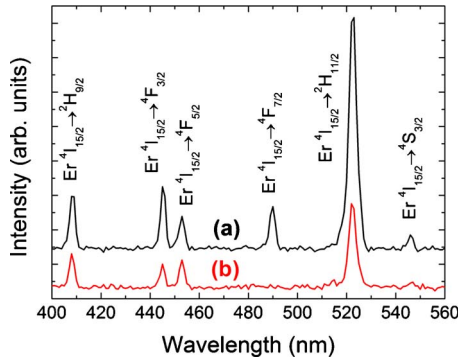


FIG. 4. (Color online) Excitation spectrum of (a): $\text{Cs}_3\text{Y}_2\text{Br}_9$; 1%Er and (b): $\text{Cs}_3\text{Y}_2\text{Br}_9$; 1%Er; 15%Yb for Er^{3+} ${}^4\text{I}_{13/2} \rightarrow {}^4\text{I}_{15/2}$ emission at 1548 nm, $T = 4.4$ K.

tween Figs. 4(a) and 4(b) is the absence of the ${}^4\text{F}_{7/2}$ peak in Fig. 4(b). Codoping with 15% Yb^{3+} in $\text{Cs}_3\text{Y}_2\text{Br}_9$; 1%Er prevents population of the Er^{3+} ${}^4\text{I}_{13/2}$ level after excitation into the Er^{3+} ${}^4\text{F}_{7/2}$ level. The complete absence of the ${}^4\text{F}_{7/2}$ peak in Fig. 4(b) shows that the energy transfer to Yb^{3+} is very efficient and the efficiency can be estimated to be over 90%, based on the comparison of Figs. 4(a) and 4(b).

To determine the efficiency of the energy transfer process more accurately, luminescence decay curves were recorded. Figure 5 shows decay curves of Er^{3+} ${}^4\text{F}_{7/2}$ emission at 491.0 nm after Er^{3+} ${}^4\text{F}_{7/2}$ laser excitation at 489.7 nm for (a): $\text{Cs}_3\text{Y}_2\text{Br}_9$; 1%Er and (b): $\text{Cs}_3\text{Y}_2\text{Br}_9$; 1%Er; 15%Yb at 4 K. The decay times are 142 μs and 7 μs , respectively. The 20 times faster decay for the weak ${}^4\text{F}_{7/2}$ emission in the codoped samples shows that the energy transfer efficiency from the ${}^4\text{F}_{7/2}$ level is $\sim 95\%$ in the sample codoped with 15% Yb^{3+} . The efficiency for the second transfer step in the downconversion process, transfer from the ${}^4\text{I}_{11/2}$ level of Er^{3+} to the ${}^2\text{F}_{5/2}$ level of Yb^{3+} is also high. In the emission spectrum no ${}^4\text{I}_{11/2}$ emission could be detected in the codoped

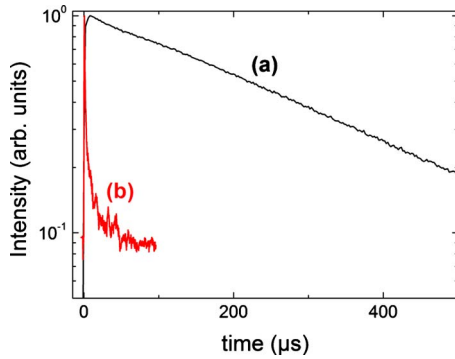


FIG. 5. (Color online) Decay curves of Er^{3+} ${}^4\text{F}_{7/2}$ emission at 491.0 nm after Er^{3+} ${}^4\text{F}_{7/2}$ excitation at 489.7 nm for (a): $\text{Cs}_3\text{Y}_2\text{Br}_9$; 1%Er and (b): $\text{Cs}_3\text{Y}_2\text{Br}_9$; 1%Er; 15%Yb for Er^{3+} $T=4.4$ K. (a) has a decay time of 142 μs , whereas (b) has a decay time of 7.4 μs .

sample [also not at low temperatures, see Fig. 2(c)]. Based on the signal-to-noise ratio and the intensity of the ${}^4\text{I}_{11/2}$ emission in the singly doped sample, the efficiency of the second transfer step is estimated over 90%. This demonstrates that the Er–Yb couple is a very efficient downconversion couple in bromides. Application in solar cells may be hampered by the hygroscopic nature of most bromides but nonhygroscopic bromides do exist and studies on downconversion with the Er–Yb couple in such bromides are underway. A second issue that needs to be addressed is the weak and spectrally narrow absorption region for the ${}^4\text{I}_{13/2} \rightarrow {}^4\text{F}_{7/2}$ transition.⁴ For efficient downconversion of a substantial part of the solar spectrum the downconversion couple needs to be combined with a sensitizer ion (e.g., Ce^{3+} or Eu^{2+}) which absorbs strongly between 350 and ~ 480 nm and transfer the energy to the ${}^4\text{F}_{7/2}$ level of Er^{3+} .

In conclusion, we have shown efficient downconversion in $\text{Cs}_3\text{Y}_2\text{Br}_9$ doped with 1% Er and 15% Yb. The low phonon frequency in bromides (180 cm^{-1}) prevents multiphonon relaxation between the various $4f$ (Ref. 11) levels of Er^{3+} and radiative decay from the $\text{Er} {}^4\text{F}_{7/2}$ level is observed. The long-lived ${}^4\text{F}_{7/2}$ level can efficiently transfer energy to two neighboring Yb^{3+} ions in $\text{Cs}_3\text{Y}_2\text{Br}_9$; 1%Er, 15%Yb. The energy level scheme shows that for both energy transfer steps the energy mismatch is small and transfer efficiencies over 95% can be determined from luminescence spectra and luminescence decay time measurements. The very high downconversion efficiency and strong Yb^{3+} emission intensity show that bromides are a promising class of materials for downconversion for the Er–Yb couple in contrast to host materials with higher phonon energies.

- ¹T. Trupke, M. Green, and P. Würfel, *J. Appl. Phys.* **92**, 4117 (2002).
- ²T. Trupke, M. Green, and P. Würfel, *J. Appl. Phys.* **92**, 1668 (2002).
- ³B. S. Richards, *Sol. Energy Mater. Sol. Cells* **90**, 1189 (2006).
- ⁴B. M. van der Ende, L. Aarts, and A. Meijerink, *Phys. Chem. Chem. Phys.* **11**, 11081 (2009).
- ⁵P. Vergeer, T. J. H. Vlugt, M. H. F. Kox, M. I. den Hertog, J. P. J. M. van der Eerden, and A. Meijerink, *Phys. Rev. B* **71**, 014119 (2005).
- ⁶Q. Zhang, C. Yang, and Y. Pan, *Appl. Phys. Lett.* **91**, 051903 (2007).
- ⁷B. M. van der Ende, L. Aarts, and A. Meijerink, *Adv. Mater.* **21**, 3073 (2009).
- ⁸L. Aarts, B. M. van der Ende, and A. Meijerink, *J. Appl. Phys.* **106**, 023522 (2009).
- ⁹L. Aarts, S. Jaeqx, and B. M. van der Ende (unpublished).
- ¹⁰S. R. Lüthi, H. U. Güdel, and M. P. Hehlen, *J. Chem. Phys.* **110**, 12033 (1999).
- ¹¹S. R. Lüthi, M. Pollnau, H. U. Güdel, and M. P. Hehlen, *Phys. Rev. B* **60**, 162 (1999).
- ¹²M. P. Hehlen, H. U. Güdel, Q. Shu, and S. C. Rand, *J. Chem. Phys.* **104**, 1232 (1996).
- ¹³M. P. Hehlen, G. Frei, and H. U. Güdel, *Phys. Rev. B* **50**, 16264 (1994).
- ¹⁴D. R. Gamelin, S. R. Lüthi, and H. U. Güdel, *J. Phys. Chem. B* **104**, 11045 (2000).
- ¹⁵L. van Pietersen, M. Heeroma, E. de Heer, and A. Meijerink, *J. Lumin.* **91**, 177 (2000).